Does a Reinforced Kinetic Macrocyclic Effect Exist? The Demetallation in Strong Acid of Copper(II) Complexes with Open and Cyclic Tetramines Containing a Piperazine Fragment

Massimo Boiocchi,[b] Marco Bonizzoni,[a] Luigi Fabbrizzi,*[a] Francesco Foti,[a] Maurizio Licchelli,[a] Antonio Poggi,[a] Angelo Taglietti,[a] and Michele Zema[c]

Dedicated to Professor Jean-Pierre Sauvage on the occasion of his 60th birthday

Abstract: The demetallation in acidic solution of the Cu^{II} complexes with open-chain and cyclic tetramines containing a piperazine unit (**2** and **3**) has been investigated in terms of its kinetic aspects and compared with the behaviour of unsubstituted counterparts (tetramines **1** and **4**). The presence of the piperazine fragment slows demetallation of the open-chain-ligand complex owing to the activation barrier associated with the conformational change from boat-to-half-boat; however, it does not affect the demetallation of the macrocyclic complex, which involves the spontaneous boat-to-twist conformational change. Thus, lateral reinforcement of a cyclam-like ligand does not add any further contribution to the typical inertness in demetallation of macrocyclic complexes.

Keywords: conformational changes · copper · kinetics · macrocycles · piperazine

Introduction

The 14-membered tetramine macrocycle cyclam (**1**) presents distinctive coordinating properties towards transition-metal ions that are not observed with noncyclic ligands and which may be exhibited to a much lesser degree by macrocycles of different atomicity and/or denticity. One of the most remarkable properties of cyclam is the inertness with respect to substitution of its metal complexes, in particular, resistance to demetallation in acidic solution, a feature that has been defined as the *kinetic macrocyclic effect*.[1]

As an example, a half-life ($t_{1/2}$) of 30 years has been estimated for the $[Ni^{II}(cyclam)]^{2+}$ complex in 1 M $HClO_4$ at 25 °C (to be compared with the corresponding complexes of noncyclic tetramines that decompose in a twinkling of an eye in an acidic solution).[2] The kinetic stability has to be ascribed to the rigidity of the macrocyclic framework and to the hindered access of hydrogen ions to the amine groups because of the closed nature of the ligand. In particular, whereas terminal amine groups of the open-chain polyamine can easily detach from the metal centre to be protonated by the hydrogen ions present in solution, this possibility is precluded for the cyclic polyamine metal complex, whose donor atoms are mechanically prevented from detaching.

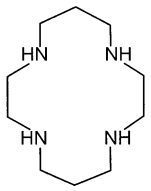

1

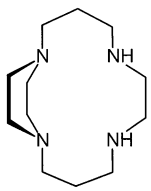

2

More recently, the so-called *reinforced* macrocycles have been introduced, namely, systems in which two amine groups are linked by a further aliphatic chain.[3] As an example, compound **2** is a *laterally reinforced* cyclam, in which two nitrogen atoms are linked by two ethylenic chains, thus giving rise to a piperazine ring. Such a ring typically displays a rich conformational activity, similar to that of cyclohexane.[4] The energy (enthalpy) diagram of the various con-

[a] Dr. M. Bonizzoni, Prof. L. Fabbrizzi, Dr. F. Foti, Prof. M. Licchelli, Prof. A. Poggi, Dr. A. Taglietti
Dipartimento di Chimica Generale
Università di Pavia
via Taramelli 12, 27100 Pavia (Italy)
Fax: (+39) 0382-528544
E-mail: luigi.fabbrizzi@unipv.it

[b] Dr. M. Boiocchi
Centro Grandi Strumenti
Università di Pavia
via Bassi 21, 27100 Pavia (Italy)

[c] Dr. M. Zema
Dipartimento di Scienze della Terra
Università di Pavia
via Ferrata 1, 27100 Pavia (Italy)

 DOI: 10.1002/chem.200305717 © 2004 Wiley-VCH Verlag GmbH & Co. KGaA, Weinheim

formers, calculated through a semiempirical method (see the Experimental Section), is reported in Figure 1.

In this work, we wished to investigate whether and to what extent possible conformational changes of the piperazine residue may affect the kinetic stability of metal com-

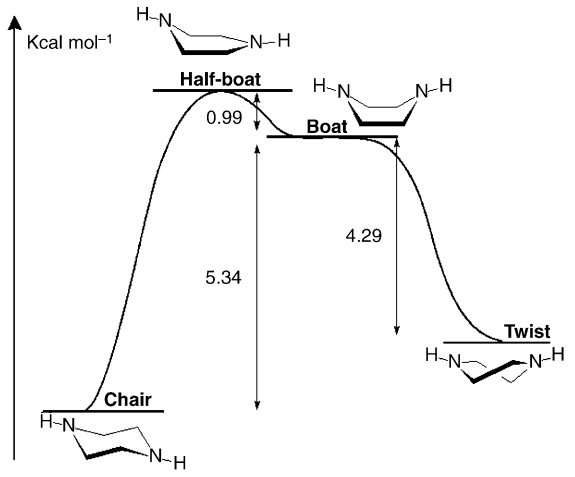

Figure 1. Energy diagram of the conformers of piperazine, calculated with a semiempirical method (PM3).

plexes with reinforced macrocycles such as **2**. However, it might have been difficult to separate the reinforcement contribution to the inertness from that arising as a consequence of the intrinsic cyclic nature of the ligand. Therefore, in order to exclude the effects arising from the cyclic nature of the ligand, our initial investigations focused on the kinetic behaviour of the complexes of a noncyclic reinforced tetramine, 3-[4-(3-aminopropyl)piperazin-1-yl]propylamine (**3**), which contains a piperazine fragment in its framework. For comparative purposes, we also considered the parent non-reinforced open-chain tetramine N^1-[2-(3-aminopropylamino)ethyl]propane-1,3-diamine (**4**).

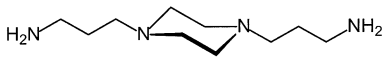

3

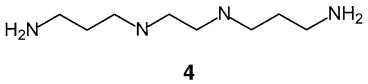

4

We report herein a kinetic investigation on the demetallation of the copper(II) complexes of **1**–**4** in acidic solution. The kinetic behaviour has been interpreted on the basis of the structural details available for Cu^{II} complexes of both **2** and **3** and for the uncomplexed protonated ligands, with a special reference to the conformation of the piperazine unit, whether *chair*, *boat* or *twist*.

Results and Discussion

Structural studies: The crystal and molecular structures of the complexes $[Cu^{II}(\mathbf{2})]^{2+}$ and $[Cu^{II}(\mathbf{3})]^{2+}$, as perchlorate salts, were determined by means of X-ray single-crystal diffraction. Selected bond lengths and bond angles are given in Table 1. Moreover, the structure of the triprotonated form of the reinforced macrocycle **2** (= L), as the tri-hydrochloride salt, $[LH_3]Cl_3$, is also reported.

Table 1. Selected bond lengths[Å] and angles[°] for the $[Cu^{II}(\mathbf{3})](ClO_4)_2$ and $[Cu^{II}(\mathbf{2})](ClO_4)_2$ complexes.

	$[Cu^{II}(\mathbf{3})](ClO_4)_2$	$[Cu^{II}(\mathbf{2})](ClO_4)_2$
Cu(1)–N(1)	2.021(7)	1.961(12)
Cu(1)–N(2)	2.018(6)	2.005(9)
Cu(1)–N(3)	1.996(7)	2.009(9)
Cu(1)–N(4)	1.999(6)	1.980(9)
N(1)-Cu(1)-N(2)	74.00(25)	77.71(48)
N(1)-Cu(1)-N(3)	171.12(23)	161.81(35)
N(1)-Cu(1)-N(4)	96.45(22)	102.20(46)
N(2)-Cu(1)-N(3)	97.90(29)	97.78(37)
N(2)-Cu(1)-N(4)	167.47(23)	169.80(35)
N(3)-Cu(1)-N(4)	91.02(26)	86.23(38)

$[Cu^{II}(\mathbf{3})](ClO_4)_2$: The ORTEP diagram of the complex is shown in Figure 2. The Cu^{II} ion has an almost square-planar coordination, with a deviation from the N(1)-N(2)-N(3)-N(4) mean plane of 0.11(1) Å. It is probably a weak Cu–O interaction with the perchlorate ion (Cu(1)–O(3) 2.544(13) Å) that induces the small pyramidal distortion for the metal centre. The mean Cu–N bond lengths are 2.019(8) and 1.997(7) for the tertiary and primary amines, respectively.

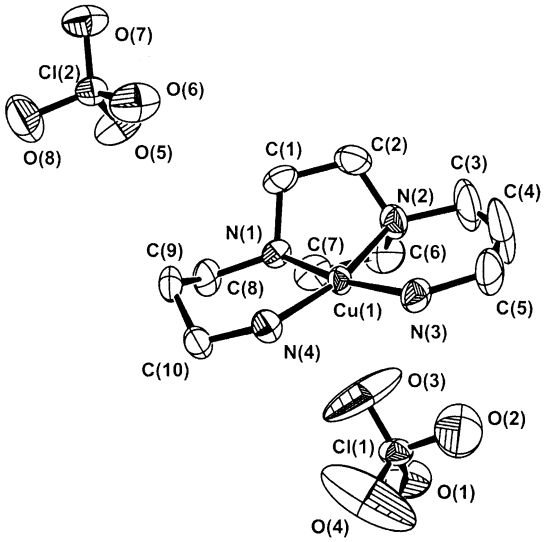

Figure 2. An ORTEP view of the $[Cu^{II}(\mathbf{3})](ClO_4)_2$ complex salt (thermal ellipsoids are drawn at the 30% probability level, hydrogen atoms are omitted for clarity). The piperazine subunit exhibits the boat conformation, while the Cu^{II} centre shows an almost square-planar coordination. Weak interaction with one perchlorate ion (Cu(1)–O(3) 2.544(13) Å) is associated with a slight pyramidal distortion of the metal centre. The C(4) thermal ellipsoid suggests positional disorder; however, refinement of two alternative C(4) positions does not improve the model (see text).

© 2004 Wiley-VCH Verlag GmbH & Co. KGaA, Weinheim

Coordination to the metal forces the piperazine unit of **3** into the less favourable boat conformation: the puckering parameters are:[5] $q_2 = 0.865(8)$ Å, $q_3 = 0.001(9)$ Å, $\phi = -2.1(7)°$, $Q_T = 0.865(8)$ Å, $\theta = 89.9(6)°$. The N(1) and N(2) atoms are placed 0.75(1) Å above the C(1)-C(2)-C(6)-C(7) best plane, while the mean deviation for the four carbon atoms is 0.02(1) Å. The N(1)–N(2) apex–apex distance is 2.431(8) Å.

The N(4)-Cu(1)-N(1)-C(8)-C(9)-C(10) chelate ring adopts a half-chair conformation. The deviations for the atoms forming the N(4)-Cu(1)-N(1)-C(8) best plane are in the range 0.03(1)–0.07(1) Å, while C(9) and C(10) are placed at 0.60(1) and 0.17(1) Å, respectively, above and below the best plane. The other hexaatomic chelate ring is characterised by positional disorder at the refined C(4) position, which shows a thermal ellipsoid that is very elongated along a direction normal to the N(3)-Cu(1)-N(2)-C(3) best plane. It is probable that the C(4) carbon atom is statistically distributed above and below its mean position, thus suggesting that the crystal is formed by molecules that have two different conformations for this hexaatomic chelate ring. Several attempts to refine two alternative positions for C(4) did not improve the agreement index, and feasible results were only obtained assuming strong geometrical constraints. On account of our failure to obtain the geometrical features of the chelate ring containing C(4), we chose to present a non-constrained model with a single mean C(4) site that is almost coplanar with the N(3)-Cu(1)-N(2)-C(3) mean plane. This model allows a better identification of the positional disorder and clearly indicates the chemically unacceptable values of the bond lengths and angles involving the C(4) position.

*[Cu^{II}(**2**)](ClO$_4$)$_2$*: The ORTEP diagram of this macrocyclic complex is reported in Figure 3. The Cu^{II} ion exhibits square-planar coordination, with a moderate tetrahedral distortion. A weak Cu–O interaction with one of the perchlorate ions is probably present (Cu(1)–O(1) 2.548(10) Å), but it is not strong enough to induce a pyramidal distortion of the complex. The Cu^{II} ion is displaced by 0.06(1) Å from the N(1)-N(2)-N(3)-N(4) mean plane; the mean metal–nitrogen distance is 1.983(10) and 1.995(9) for tertiary and secondary amine groups, respectively. However, the four nitrogen atoms are not perfectly coplanar, their deviations from the best plane are in the range 0.22(1)–0.24(1) Å. In particular, they are alternatively placed above and below the mean plane, thus giving rise to a slight tetrahedral distortion of the square-planar Cu^{II} coordination. Such a distortion is not present in the previously discussed [Cu^{II}(**3**)](ClO$_4$)$_2$ complex (in which the four N atoms deviate, on average, by 0.03(1) Å from the best plane displaced by 0.11(1) Å from the metal centre). Moreover, no distortion is observed in the corresponding complex of plain cyclam, [Cu^{II}(**1**)]$^{2+}$,[6] in which the metal centre is perfectly coplanar with the four secondary nitrogen atoms and the two perchlorate ions are symmetrically located along the *z* axis, at a distance of 2.57 Å.

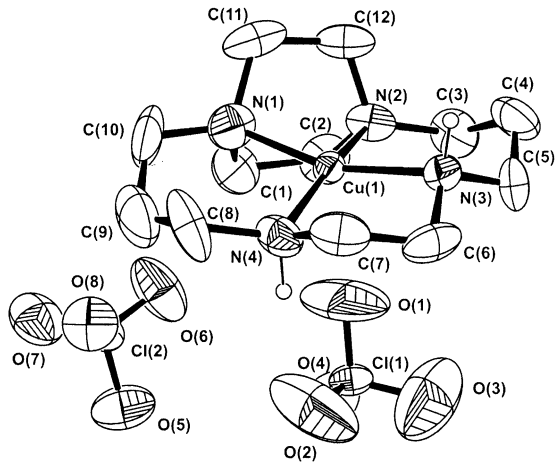

Figure 3. An ORTEP view of the [Cu^{II}(**2**)](ClO$_4$)$_2$ complex salt (thermal ellipsoids are drawn at the 30% probability level, only hydrogen atoms bonded to the secondary amines are shown). The piperazine ring is in the boat conformation; however, a slight twisting of the regular boat conformation is observed. The Cu^{II} centre exhibits tetrahedrally distorted square-planar coordination. A slightly short Cu^{II}–O distance is also observed (Cu(1)–O(1) 2.548(10) Å).

The crystal structures of copper(II) complexes with laterally reinforced cyclam derivatives have been recently reported by Kaden et al.[7] In the two complexes of *N,N′,N″,N‴*-tetraalkyl-substituted macrocycles bearing either methyl or ethyl substituents on N(3) and N(4) atoms, the geometry of the metal centre is definitely square-pyramidal, with a water molecule occupying the apical position. In both complexes, the Cu–O(water) distance is relatively short (Cu–O 2.23–2.24 Å).

On the other hand, in the laterally reinforced macrocycle with an alkyl substituent only on one of the two remaining nitrogen atoms (donor set: 3 tertiary nitrogen atoms, 1 secondary),[7] a tetrahedrally distorted square-planar geometry is observed. This situation is very similar to that found for the [Cu^{II}(**2**)](ClO$_4$)$_2$ complex (i.e., in presence of two tertiary amines and two secondary amines). Thus, it appears that moving from two or three to four tertiary amine nitrogen atoms in a 14-membered laterally reinforced macrocycle induces the change from a square-planar, even if tetrahedrally distorted, to a square-pyramidal geometry.

In the [Cu^{II}(**2**)](ClO$_4$)$_2$ complex, the piperazine ring exhibits a boat conformation: the puckering parameters are:[5] $q_2 = 0.882(7)$ Å, $q_3 = 0.026(8)$ Å, $\phi = 9.32(6)°$, $Q_T = 0.882(7)$ Å, $\theta = 88.3(5)°$. The ϕ value indicates a slight twisting of the regular boat conformation (in which $\phi = 0°$). The N(1) and N(2) atoms deviate from the C(1)-C(2)-C(11)-C(12) best plane by 0.78(1) and 0.73(1) Å, respectively. The four carbon atoms are displaced, on average, by 0.07(1) Å from the mean plane. The N(1)–N(2) apex–apex distance is 2.461(9).

It has to be noted that in the previously mentioned complexes of *N*-alkyl-substituted derivatives of **2**,[7] the piperazine ring shows a regular boat conformation when the metal coordination is square pyramidal (i.e., in presence of only tertiary amines), while the piperazine unit is slightly distorted towards the more stable twist–boat conformation, when the complex presents a tetrahedrally distorted square-planar

 © 2004 Wiley-VCH Verlag GmbH & Co. KGaA, Weinheim

geometry (i.e., when one or more secondary amine groups are present).

Noticeably, for such different geometrical details, significant differences in the spectral features are observed: the $[Cu^{II}(\mathbf{1})]^{2+}$ complex has a d–d absorption band with $\lambda_{max}=$ 500 nm, whereas that of $[Cu^{II}(\mathbf{2})]^{2+}$ is at 525 nm. The energy of the band is a measure of the intensity of the metal–ligand interactions and they are stronger in the $[Cu^{II}(\mathbf{1})]^{2+}$ complex, in which the metal is chelated by the four nitrogen atoms in a coplanar conformation. On the other hand, the less symmetric $[Cu^{II}(\mathbf{2})]^{2+}$ complex exhibits a higher molar absorbance ($\varepsilon=255\,M^{-1}cm^{-1}$) compared to the perfectly square-planar $[Cu^{II}(\mathbf{1})]^{2+}$ complex ($\varepsilon=77\,M^{-1}cm^{-1}$).

In the $[Cu^{II}(\mathbf{2})]^{2+}$ complex, the two hexaatomic chelate rings adopt two opposite half-chair conformations in which the C(4) and C(9) vertices point in opposite directions. As far as the N(1)-Cu(1)-N(4)-C(8)-C(9)-C(10) hexaatomic ring is concerned, the deviations for the atoms forming the N(4)-Cu(1)-N(1)-C(10) best plane are in the range 0.02(1)–0.05(1) Å; C(8) and C(9) are respectively placed 0.18(1) and 0.44(1) Å above and below the best plane. The other six-membered chelate ring shows deviations for the atoms forming the N(3)-Cu(1)-N(2)-C(3) best plane in the range 0.06(1)–0.15(1) Å; C(4) is placed 0.44(1) Å above the mean plane, while C(5) is 0.32(1) Å below the mean plane. The five-membered chelate ring adopts a twisted conformation: C(6) and C(7) are located above and below the Cu(1)-N(3)-N(4) plane with deviations of 0.32(1) and 0.38(1) Å, respectively.

$[LH_3]Cl_3$: The ORTEP diagram of the triprotonated form of the reinforced macrocycle **2** is shown in Figure 4. The piperazine subunit is not in the more stable chair conformation, but in the less energetically favourable twist–boat conformation. The puckering parameters are:[5] $q_2=0.806(6)$ Å, $q_3=0.012(5)$ Å, $\phi=26.7(3)°$, $Q_T=0.807(6)$ Å, $\theta=89.1(4)°$. All the four carbon atoms deviate from the C(1)-C(2)-C(11)-C(12) best plane by 0.18(1) Å. The N(1) and N(2) atoms are displaced from the best plane by 0.64(1) Å and 0.61(1) Å, respectively. The N(1)–N(2) apex–apex distance is 2.645(5) Å. Interestingly, also in the previously investigated diprotonated form of a laterally reinforced macrocycle bearing two ethyl substituents on the two remaining nitrogen atoms, the piperazine fragment is present in the twist–boat conformation.[7]

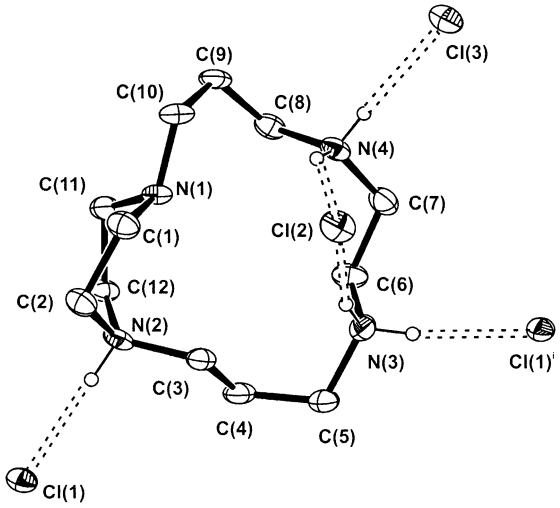

Figure 4. An ORTEP view of the $[LH_3]Cl_3$ salt: thermal ellipsoids are drawn at the 30% probability level, only hydrogen atoms bonded to the protonated amines are shown. Dashed lines show the N–H···Cl interactions. Symmetry code: i $=-x+\frac{1}{2}, -y, z+\frac{1}{2}$. The piperazine ring is in the twist–boat conformation.

The protonated amine nitrogen atoms show the longest C–N bond length: the mean bond values are 1.490(9) Å for the secondary amines and 1.494(8) Å for the tertiary amine. The mean C–N bond length for the nonprotonated N(1) nitrogen is 1.459(8) Å.

All protonated amines are involved in N–H···Cl interactions [N(2)···Cl(1) 3.084(5) Å, H(13)···Cl(1) 2.197(51) Å, N(2)–H(13)···Cl(1) 173.3(45)°, N(3)···Cl(2) 3.128(6) Å, H(14B)···Cl(2) 2.267(60) Å, N(3)–H(14B)···Cl(2) 162.7(50)°, N(3)···Cl(1)^{i} 3.139(5) Å, H(14A) ···Cl(1)^{i} 2.255(40), N(3)–H(14A)···Cl(1)^{i} 170.9(29)°, symmetry code: i $=-x+\frac{1}{2}, -y, z+\frac{1}{2}$, N(4)···Cl(2) 3.048(5) Å, H(15A)···Cl(2) 2.276(71) Å, N(4)–H(15A)···Cl(2) 144.6(55)°, N(4)···Cl(3) 3.058(5), H(15B)···Cl(3) 2.198(57), N(4)–H(15B)···Cl(3) 162.1(51)°].

In particular, while the Cl(2) anion allows the occurrence of an intramolecular N-H···Cl interaction, the Cl(1) anion connects two adjacent molecules: it forms hydrogen bonds to the N(2) and N(3) atoms from different molecules. These intermolecular hydrogen bridges, with van der Waals forces, are responsible for the stability of the crystal.

Kinetic aspects of demetallation in acidic solution: Demetallation processes of Cu^{II} complexes with open-chain tetramines **3** and **4** were studied by stopped-flow spectrophotometric investigations. In a typical experiment, one of the syringes contained a solution of the copper complex, adjusted to the minimum pH which ensured its highest concentration. This value was calculated from the equilibrium constants available for Cu^{II} complexes of **3**[9] and **4**.[10] The other syringe contained perchloric acid in different concentrations. In all cases, the solution was adjusted to the desired ionic strength (0.5 M) with $NaClO_4$. The temperature was maintained at 25 °C.

Demetallation of $[Cu^{II}(\mathbf{3})]^{2+}$ was investigated first. The concentration of the metal complex varied between 6×10^{-5} and 1.3×10^{-3} M, and the pH was adjusted to 7.0. This solution was mixed in the stopped-flow chamber with solutions containing a variable quantity of $HClO_4$ (from 5×10^{-4} M to 0.1 M). In each experiment, the absorbance of a band at $\lambda=$ 300 nm (LMCT in nature) was monitored and the linear dependence of the logarithm of the corrected absorbance versus time was found in all cases. The slope of the least-squares straight line gave the value of k_{obs}. It was found that the values of k_{obs} remained constant over the investigated interval of $[H^+]$, $k_{obs}=0.16\pm0.02\,s^{-1}$. This behaviour can be tentatively explained according to the decomplexation scheme illustrated in Scheme 1.

In the first step, a terminal primary amine group is protonated, and this process is regulated by an equilibrium constant K_H. Then, the adjacent tertiary nitrogen atom detaches

 © 2004 Wiley-VCH Verlag GmbH & Co. KGaA, Weinheim

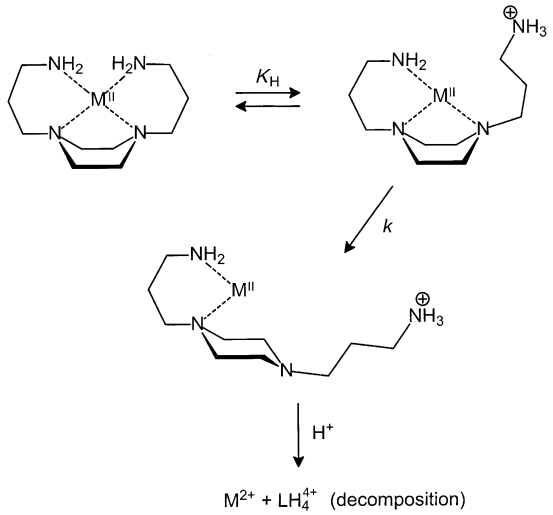

Scheme 1. Hypothesised mechanism for the decomposition of the $[Cu^{II}(\mathbf{3})]^{2+}$ complex in acid. The rate-determining step (regulated by k) is attributed to the decomplexation of one of the tertiary amine groups of the piperazine fragment, a process which corresponds to the boat-to-chair conversion.

according to a process controlled by the rate constant k. Under these circumstances, k_{obs} should be expressed by Equation (1):

$$k_{obs} = \frac{kK_H[H^+]}{1 + K_H[H^+]} \quad (1)$$

The fact that k_{obs} was found to be independent of $[H^+]$ indicates that $K_H[H^+] \gg 1$. As a consequence, $k_{obs} = k = 0.16\ s^{-1}$, corresponding to a lifetime τ of 6.2 ± 0.7 s. Indeed, on addition of strong acid to a test tube containing a solution of $[Cu^{II}(\mathbf{3})]^{2+}$, the persistence of the blue colour of the copper(II) polyamine complex can be visually perceived for several seconds.

Analogous studies were carried out on a 0.5 M $NaClO_4$ solution of the $[Cu^{II}(\mathbf{4})]^{2+}$ complex. In the present case, the value of k_{obs} was found to increase over the explored interval of $[H^+]$, according to the profile shown in Figure 5.

We can tentatively assume that the decomplexation mechanism illustrated in Scheme 1 also holds for the $[Cu^{II}(\mathbf{4})]^{2+}$ complex. Indeed, nonlinear least-squares treatment of k_{obs} values fitted Equation (1) quite well (see the solid line in Figure 5), and gave the following parameters: $K_H = 72 \pm 5$ and $k = 13.4 \pm 1.7\ s^{-1}$. Dependence of k_{obs} upon $[H^+]$ has to be ascribed to the relatively low value of K_H: this reflects the rather strong interaction between Cu^{II} and the terminal primary amine group. Such an interaction is distinctly weaker for the $[Cu^{II}(\mathbf{3})]^{2+}$ complex. However, the most important difference concerns the rate constant k, whose value is almost two orders of magnitude higher than that observed for the piperazine-containing complex. In particular, the lifetime τ of $[Cu^{II}(\mathbf{4})]^{2+}$ in a strongly acidic solution is 75 ± 9 ms; this means that the blue colour of the complex, on addition of acid, disappears in the twinkling of an eye, as usually observed with copper(II) complexes with open-chain tetramines. The different kinetic behaviour of the two complexes has to be ascribed to the conformational changes of the piperazine fragment that occur during the demetallation process of the $[Cu^{II}(\mathbf{3})]^{2+}$ complex. In fact, structural studies have shown that the piperazine fragment adopts a regular boat conformation in the $[Cu^{II}(\mathbf{3})]^{2+}$ complex. On the other hand, there is plenty of structural evidence showing that the piperazine unit assumes the energetically more favourable chair conformation in the protonated forms of uncomplexed **3**.[11]

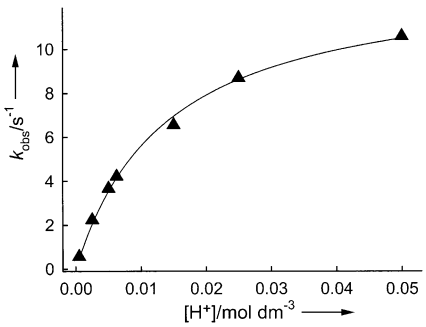

Figure 5. The dependence of k_{obs} upon $[H^+]$ for the decomposition of $[Cu^{II}(\mathbf{4})]^{2+}$ in acid. —— is the least-squares curve fitted on Equation (1).

In this context, it has to be noted that as the piperazine fragment changes from the boat to the more stable chair conformation, it has to pass through the more energetic half-boat conformation, which corresponds to the transition state (see Figure 1 for the energy profile). Thus, the relatively low value of k reflects the energy barrier to be overcome during the decomplexation process of **3**. Evidently, ligand **4**, in which the two secondary amine groups are joined only by an ethylenic chain, does not have to overcome such an energy barrier.

Therefore, the presence of a piperazine fragment in the ligand framework imparts extra kinetic stability to its transition-metal complexes, namely, with Cu^{II}. At this stage, it seemed interesting to verify whether such a conformational effect also operates with cyclic ligands, such as **2**, which contains a piperazine unit, thus conveying additional stability to demetallation in addition to the usual macrocyclic effect.

On this basis, we carried out a kinetic investigation of the demetallation of macrocyclic $[Cu^{II}(\mathbf{1})]^{2+}$ and $[Cu^{II}(\mathbf{2})]^{2+}$ complexes in acidic solution. Evidently, in view of the typical macrocyclic inertness, such a study would not be carried out with a stopped-flow apparatus. Moreover, the process is indeed so slow that, in order to complete the experiments within a reasonable time, these were carried out at a distinctly higher temperature. In particular, two screw-capped bottles containing 50 mL of an aqueous 1 M $HClO_4$ solution, one with 1.350×10^{-3} M of $[Cu^{II}(\mathbf{2})]^{2+}$ and the other with 1.089×10^{-3} of $[Cu^{II}(\mathbf{1})]^{2+}$, were kept in a thermostat at 60 °C and the absorbance of the corresponding d–d bands was measured at regular intervals over a period of one month and longer.

Figure 6a shows the decay of the absorption band of the $[Cu^{II}(\mathbf{1})]^{2+}$ complex, while in Figure 6b the logarithm of the absorbance (Abs) is plotted versus time. Satisfactory linear fitting indicates pseudo-first-order behaviour and the slope

 © 2004 Wiley-VCH Verlag GmbH & Co. KGaA, Weinheim

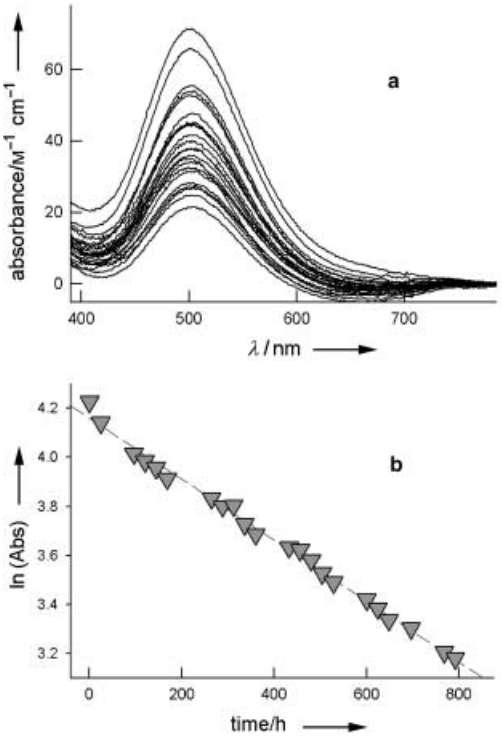

Figure 6. a) Spectra of a solution of $[Cu^{II}(\mathbf{1})]^{2+}$ in 1 M $HClO_4$, at 60 °C taken at regular intervals over a period of ≈1 month. b) Linear plot of the natural logarithm of the molar absorbance at 500 nm versus time, whose slope gives $k_{obs} = 1.31 \pm 0.12 \times 10^{-3}\ h^{-1}$.

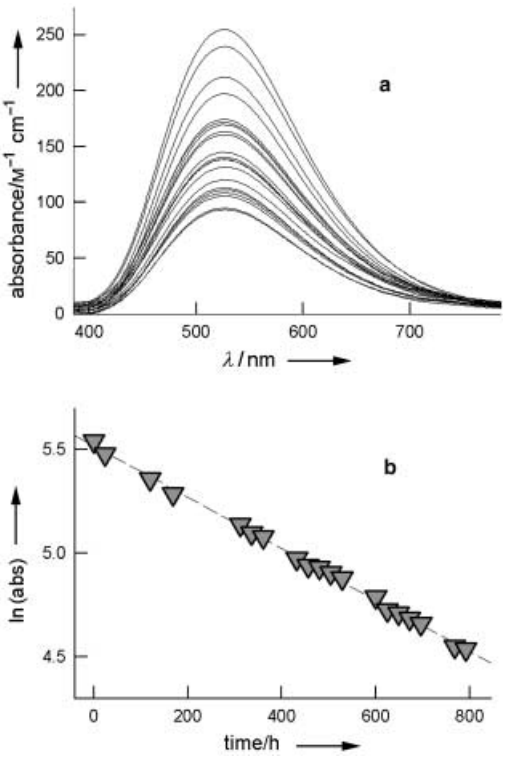

Figure 7. a) Spectra of a solution of $[Cu^{II}(\mathbf{2})]^{2+}$ in 1 M $HClO_4$, at 60 °C taken at regular intervals over a period of ≈1 month. b) Linear plot of the natural logarithm of the molar absorbance at 525 nm versus time, whose slope gives $k_{obs} = 1.23 \pm 0.11 \times 10^{-3}\ h^{-1}$.

of the least-squares straight line gives a k_{obs} of $1.31 \pm 0.12 \times 10^{-3}\ h^{-1}$, to which a $t_{1/2}$ of 22.0 ± 2.0 days corresponds. On the other hand, the decay of the d–d band of the $[Cu^{II}(\mathbf{2})]^{2+}$ complex is shown in Figure 7a, while Figure 7b displays the plot of linear log(Abs) versus time, which gives $k_{obs} = 1.23 \pm 0.11 \times 10^{-3}\ h^{-1}$ and $t_{1/2} = 23.5 \pm 2.1$ days.

Thus, it appears that the two complexes have a comparable kinetic stability with respect to demetallation in acidic solution and that, in particular, the presence of a piperazine ring has no effect on the inertness of the $[Cu^{II}(\mathbf{2})]^{2+}$ complex. This apparently surprising behaviour can be accounted for on the basis of the structure of the uncomplexed macrocycle **2**, in its triprotonated form (Figure 4). It can be seen that the piperazine ring adopts a twist conformation. The available data do not allow us to propose a detailed mechanism for the protonation–demetallation process. Clearly, the $[LH_3]^{3+}$ species (L = **2**) is present in the sequence of products which form after the metal has been removed from the macrocycle. Most importantly, the demetallation process involves the boat (in the complex) to twist (in the protonated macrocycle) conversion. The energy profile shown in Figure 1 indicates that this conformational change is spontaneous and is not affected by any energy barrier. Thus, the conformational change of the piperazine ring that occurs during demetallation of the $[Cu^{II}(\mathbf{2})]^{2+}$ complex does not introduce any additional energy barrier and the kinetic behaviour is the same as for the reference macrocyclic complex $[Cu^{II}(\mathbf{1})]^{2+}$. Accordingly, the kinetic stability of $[Cu^{II}(\mathbf{2})]^{2+}$ in acid is solely related to the cyclic nature of the ligand and, therefore, cannot be different from that of the complex of plain cyclam, $[Cu^{II}(\mathbf{1})]^{2+}$.

Conclusion

This work has demonstrated that the presence of a piperazine fragment within a tetramine ligand may have relevant effects on the kinetic stability of the corresponding transition metal complexes. Such effects derive from the rich conformational behaviour of the cyclohexane-like heterocycle. In particular, the demetallation of the complex with a piperazine-containing tetramine (e.g. **3**) involves the conformational change from boat to chair, which implies the endothermic transition through the half-boat intermediate. As a consequence, the presence of the piperazine fragment imparts a perceivable inertness with respect to the demetallation. On the other hand, in the case of cyclic ligands, such as **2**, demetallation involves the conformational change from boat to twist, which is not affected by any activation barrier. Thus, the presence of a piperazine fragment does not impart any additional kinetic stability to the typically inert macrocyclic complexes. In conclusion, as far as laterally reinforced macrocycles, such as **2**, are concerned, a reinforced kinetic macrocyclic effect does not exist.

© 2004 Wiley-VCH Verlag GmbH & Co. KGaA, Weinheim

Experimental Section

Synthesis of ligands and complexes: Cyclam **1** was obtained by means of Barefield's procedure.[12] Open-chain tetramines **3** and **4** were purchased (Sigma-Aldrich) and were used without further purification for the synthesis of copper(II) complexes. The laterally reinforced macrocycle **2** was obtained through a modification of a reported procedure,[13] as illustrated in Scheme 2.

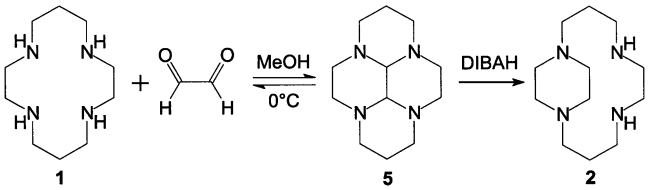

Scheme 2. Synthetic route to the laterally reinforced macrocycle **2**.

Decahydro-3a,5a,8a,10a-tetraazapyrene (5): Aqueous 40% glyoxal (1.16 g, 8 mmol) in methanol (8 mL) was added dropwise to a solution of **1** (1.6 g, 2 mmol) in methanol (60 mL) at 0°C. The reaction was over immediately. The mixture was stirred at 0°C for 30 min. The solvent was evaporated, and the residue was purified by chromatography (Al_2O_3, CH_2Cl_2:MeOH:NH_3, 95/5/0.5) to give **5** (1.77 g, 97% yield) as light yellow crystals. MS: m/z: 223.2 $[M+H]^+$.

1,5,8,12-Tetraazabicyclo[10.2.2]hexadecane (2): Diisobutyl aluminium hydride (DIBAH, 75 mmol) in toluene (50 mL) was added dropwise to tetramine **5** (0.555 g, 2.5 mmol) at 0°C, and the resulting solution was allowed to warm to 25°C. This solution was refluxed for 4 d. The reaction was worked up in the usual manner: the reaction mixture was cooled at 0°C, and benzene (150 mL), sodium fluoride (12.5 g) and water (4 mL) were added. This caused the precipitation of aluminates, which were discarded by filtration and washed with ethanol. The obtained solution was concentrated in a rotary evaporator, and the obtained oil was purified by column chromatography (Al_2O_3, CH_2Cl_2:MeOH:NH_3, 100/10/1) to give **2** (522.8 mg, 93% yield), as a colourless oil. MS: m/z: 227.2 $[M+H]^+$.

Copper(II) complexes: These were obtained from the reaction of the perchlorate salt with the tetramine, either cyclic or open-chain, in methanol. The mixture was refluxed for 2 h, and a violet or red precipitate formed. The solid was filtered, washed with cold methanol and dried (yields were in the 90–95% range). The microcrystalline products were characterised by means of satisfactory elemental analysis. Crystals suitable for X-ray diffraction analysis were obtained by diffusion of diethyl ether into a solution of the complexes in methanol.

X-ray crystallographic studies: Crystal data for complexes $[Cu^{II}(\mathbf{3})](ClO_4)_2$ and $[Cu^{II}(\mathbf{2})](ClO_4)_2$ and for the triprotonated $[LH_3]Cl_3$ salt (L = **2**) are reported in Table 2.

Intensity data were collected with conventional diffractometers: a Philips PW1100 was used for the Cu^{II} complexes and an Enraf-Nonius CAD4 for the $[LH_3]Cl_3$ salt. For both instruments, the incident radiation was graphite-monochromatized $Mo_{K\alpha}$ ($\lambda = 0.71073$ Å). Data was collected at ambient temperature with $\omega-2\theta$ scan type. Data reduction (including intensity integration, background, Lorentz and polarization corrections) was performed with local programs (for the data collected with the Philips PW1100) and with the WinGX package (for the data collected with the CAD4).[14] Absorption corrections were calculated with the psi-scan procedure.[15] Crystal structures were solved by direct methods (SIR97)[16] and refined by a full-matrix least-square procedure on F^2 (SHELXL97).[17] Anisotropic displacement parameters were used for all non-hydrogen atoms. Hydrogen atoms in the complexes were added at calculated positions and refined with a riding model; for $[LH_3]Cl_3$ salt, hydrogen atoms bonded to the protonated amines were located in the difference Fourier maps and refined with restraints on the N–H distance.

CCDC-223834, CCDC-223835, CCDC-223836 contain the supplementary crystallographic data for this paper. These data can be obtained free of charge via www.ccdc.cam.ac.uk/conts/retrieving.html (or from the Cambridge Crystallographic Data Centre, 12 Union Road, Cambridge CB2 1EZ, UK; fax: (+44) 1223-336033; or deposit@ccdc.cam.uk).

Table 2. Crystal data for the investigated crystals.

	$[Cu^{II}(\mathbf{3})](ClO_4)_2$	$[Cu^{II}(\mathbf{2})](ClO_4)_2$	$[LH_3]Cl_3$, L = **2**
formula	$C_{10}H_{24}Cl_2CuN_4O_8$	$C_{12}H_{26}Cl_2CuN_4O_8$	$C_{12}H_{29}Cl_3N_4$
M_r	462.77	488.81	335.74
colour	blue-violet	red	colourless
crystal system	monoclinic	orthorhombic	orthorhombic
space group	$P2_1/c$ (no. 14)	$P2_12_12_1$ (no. 19)	$P2_12_12_1$ (no. 19)
a [Å]	8.900(25)	13.045(7)	9.178(2)
b [Å]	14.981(15)	14.774(4)	10.841(4)
c [Å]	14.960(35)	10.083(4)	16.808(5)
β [°]	113.31(10)	–	–
V [Å^3]	1831.8(84)	1943.3(15)	1672.4(8)
Z	4	4	4
ρ_{calcd} [g cm^{-3}]	1.68	1.67	1.33
$\mu Mo_{K\alpha}$ [mm^{-1}]	1.53	1.45	0.54
measured reflns	6527	3771	3764
unique reflns	3340	1967	2947
θ range [°]	2–25	2–25	2–25
R_{int}[a]	0.039	0.023	0.122
observed data $[I_o > 2\sigma(I_o)]$	2273	1635	2711
$R1$, $wR2$ (obsd data)[b]	0.065, 0.182	0.065, 0.173	0.089, 0.222
$R1$, $wR2$ (all data)[b]	0.097, 0.207	0.076, 0.186	0.095, 0.233
GOF[c]	1.06	1.05	1.11
parameters	226	245	180

[a] $R_{int} = \Sigma|F_o^2 - F_o^2(mean)|/\Sigma F_o^2$; [b] $R1 = \Sigma||F_o| - |F_c||/\Sigma|F_o|$, $wR2 = [\Sigma[w(F_o^2 - F_c^2)^2]/[w(F_o^2)^2]]^{1/2}$, where $w = 1/[\sigma^2 F_o^2 + (aP)^2 + bP]$ and $P = [(\max(F_o^2, 0) + 2F_c^2]/3$; [c] $GOF = [\sigma[w(F_o^2 - F_c^2)^2]/(n-p)]^{1/2}$, where n is the number of reflections and p the total number of refined parameters.

Kinetic studies: Kinetic studies of the demetallation of $[Cu^{II}L]^{2+}$ (L = **3**, **4**) in acidic solution were performed with a high-speed diode-array spectrophotometer coupled to a stopped-flow system. The spectrophotometer was a TIDAS (Transputer Integrated Diode Array System) apparatus, manufactured by J&M GmbH, Aalen (Germany). The 512-diode array can acquire a 512 point spectrum (λ = 200–620 nm) in a time as short as 1.3 ms, with a wavelength resolution of 0.8 nm. Up to 1000 spectra can be acquired and stored in the memory of the transputer board. The stopped-flow module (SMF-3, Bio-Logic, Claix, France) used with the spectrophotometer consisted of a three-syringe system with two mixers. The three syringes were driven by independent stepping motors, operating at 6400 steps per motor turn. The observation chamber was a quartz cuvette with an optical path of 5 mm (SMF-3TC-50/10). The movement of the syringes, the flow rate, the flow stop and fast spectral acquisition were controlled by a personal computer by means of dedicated software. The SMF-3 module was thermostatted at 25.0°C by circulating water. In a typical experiment, syringe 1 contained a $[Cu^{II}L](ClO_4)_2$ solution, adjusted to the desired pH and to constant ionic strength with $NaClO_4$, and syringe 2 contained an $HClO_4$ solution, adjusted to a constant ionic strength with $NaClO_4$. The flow rate of each syringe was 4.00 mL s^{-1}, thus, the total flow rate after mixing was 8.00 mL s^{-1}. At this flow rate, the time the solution took to travel from the mixer to the observation chamber (dead time) was $\approx$3 ms.

For L = **1**, **2**, spectra of the solutions of the Cu^{II} complexes in 1 M $HClO_4$ were measured at regular time intervals with a VARIAN Cary 100 Scan spectrophotometer. A 2 mL aliquot of the solution was taken from a 50 mL screw-capped bottle kept in the thermostat. The aliquot was placed in the cuvette for measurement, and then returned to the bottle.

Semiempirical calculations: All the calculations reported were carried out with the semiempirical PM3 method.[18] The chair–boat transition state geometry was determined by a quadratic synchronous transit method,[19] with the PM3-optimised chair and boat structures as endpoints. The positions of the NH hydrogens in the considered conformers were derived from the crystal structures obtained for ligands and complexes: in short, the *eq,eq-chair* conformer was derived from structures of

 © 2004 Wiley-VCH Verlag GmbH & Co. KGaA, Weinheim

the fully protonated open-chain tetramine **3**,[11] the *eq*,*eq-boat* from the structure of the Cu^{II} complexes of **2** and **3**, and the *ax*,*eq-twist* from the structure of the uncomplexed triply protonated ligand **2**.

Acknowledgments.

Financial support by the European Union (RTN Contract HPRN-CT-2000–00029) and of the Italian Ministry of University and Research (PRIN 2001 Dispositivi Supramolecolari and FIRB Manipolazioni molecolari per macchine nanometriche, contract no. RBNE019H9K 002) is gratefully acknowledged.

[1] D. K. Cabbiness, D. W. Margerum, *J. Am. Chem. Soc.* **1970**, *92*, 2151.
[2] E. J. Billo, *Inorg. Chem.* **1984**, *23*, 236.
[3] T. J. Hubin, J. M. McCormick, S. R. Collinson, M. Buchalova, C. M. Perkins, N. W. Alcock, P. K. Kahol, A. Raghunathan, D. H. Busch, *J. Am. Chem. Soc.* **2000**, *122*, 2512, and references therein.
[4] E. L. Eliel, S. H. Wilen, *Stereochemistry of Organic Compounds*, Wiley, New York, **1994**, p. 689.
[5] D. Cremer, J. A. Pople, *J. Am. Chem. Soc.*, **1975**, *97*, 1354.
[6] P. A. Tasker, L. Skalar, *J. Cryst. Mol. Struct.* **1975**, *5*, 329.
[7] R. Kowalliek, M. Neuburger, M. Zehnder, T. A. Kaden, *Helv. Chim. Acta* **1997**, *80*, 948.
[8] G. Kickelbick, T. Pintauer, K. Matijaszwski, *New. J. Chem.* **2002**, *26*, 462.
[9] R. D. Hancock, M. P. Ngwenya, A. Evers, P. W. Wade, J. C. A. Boeyens, S. M. Dobson, *Inorg. Chem.* **1990**, *29*, 264.
[10] P. Paoletti, L. Fabbrizzi, R. Barbucci, *Inorg. Chem.* **1973**, *12*, 1861.
[11] a) T. N. Mali, R. D. Hancock, J. C. A. Boeyens, E. L. Oosthuizen, *J. Chem. Soc. Dalton Trans.* **1991**, 1161; b) V. Soghomonian, Q. Chen, Y. Zhang, R. C. Haushalter, C. J. O'Connor, C. Tao, J. Zubieta, *Inorg. Chem.* **1995**, *34*, 3509.
[12] E. K. Barefield, E. Wagner, A. W. Herlinger, A. R. Dahl, *Inorg. Synth.* **1976**, *16*, 220.
[13] H. Yamamoto, K. Maruoka, *J. Am. Chem. Soc.* **1981**, *103*, 4186.
[14] L. J. Farrugia, *J. Appl. Crystallogr.* **1999**, *32*, 837.
[15] A. C. T. North, D. C. Phillips, F. S. Mathews, *Acta Crystallogr.* **1968**, *24*, 351.
[16] A. Altomare, M. C. Burla, M. Camalli, G. L. Cascarano, C. Giacovazzo, A. Guagliardi, A. G. G. Moliterni, G. Polidori, R. Spagna, *J. Appl. Crystallogr.* **1999**, *32*, 115.
[17] G. M. Sheldrick, SHELX 97 Programs for Crystal Structure Analysis. University of Göttingen (Germany), **1998**.
[18] J. J. P. Stewart, *J. Comput. Chem.* **1989**, *10*, 209; J. J. P. Stewart, *J. Comput. Chem.* **1989**, *10*, 221.
[19] C. Peng, H. B. Schlegel, *Israel J. Chem.* **1993**, *33*, 449.

Received: November 11, 2003

Published online: April 29, 2004

 © 2004 Wiley-VCH Verlag GmbH & Co. KGaA, Weinheim